Electronic Supplementary Material (ESI) for Dalton Transactions.

Supplementary Information

Gold Nanoparticles Functionalised with Fast Water Exchanging Gd^{3+} Chelates: Linker Effects on the Relaxivity

Miguel F. Ferreira,[a] Janaina Gonçalves,[a] B. Mousavi,[b] M. I. M. Prata,[c] S. P. J. Rodrigues,[d] Daniel Calle,[e] Pilar López-Larrubia,[e] Sebastian Cerdan,[e] Tiago B. Rodrigues,[f,g] Paula M. Ferreira,[a] L. Helm,[b*] José A. Martins[a*] and Carlos F. G. C. Geraldes[h]

[a]Centro de Química, Campus de Gualtar, Universidade do Minho, 4710-057 Braga, Portugal. E-mail: jmartins@quimica.uminho.pt

[b]Laboratoire de Chimie Inorganique et Bioinorganique, Ecole Polytechnique Fédérale de Lausanne, EPFL-BCH CH-1015 Lausanne, Switzerland. E-mail: lothar.helm@epfl.ch; Fax: +41 (0)21 693 98 95;Tel: +41 (0)21 693 98 76

[c]IBILI and ICNAS, Universidade de Coimbra, Coimbra, Portugal.

[d]Center of Chemistry and Department of Chemistry, University of Coimbra, 3004-535, Coimbra, Portugal.

[e]Instituto de Investigaciones Biomédicas "Alberto Sols", CSIC-UAM, Madrid, Spain

[f]Cancer Research UK Cambridge Research Institute, Li Ka Shing Centre, Cambridge CB2 0RE, United Kingdom.

[g]Department of Biochemistry, University of Cambridge, Cambridge CB2 1GA, United Kingdom.

[h]Department of Life Sciences, Faculty of Science and Technology, University of Coimbra, P.O. Box 3046, 3001-401 Coimbra, Portugal.

Corresponding authors:

José A. Martins, Centro de Química, Campus de Gualtar, Universidade do Minho, 4710-057 Braga, Portugal.

Lothar Helm, Ecole Polytechnique Féderale de Lausanne, EPFL-BCH CH-1015 Lausanne, Switzerland.

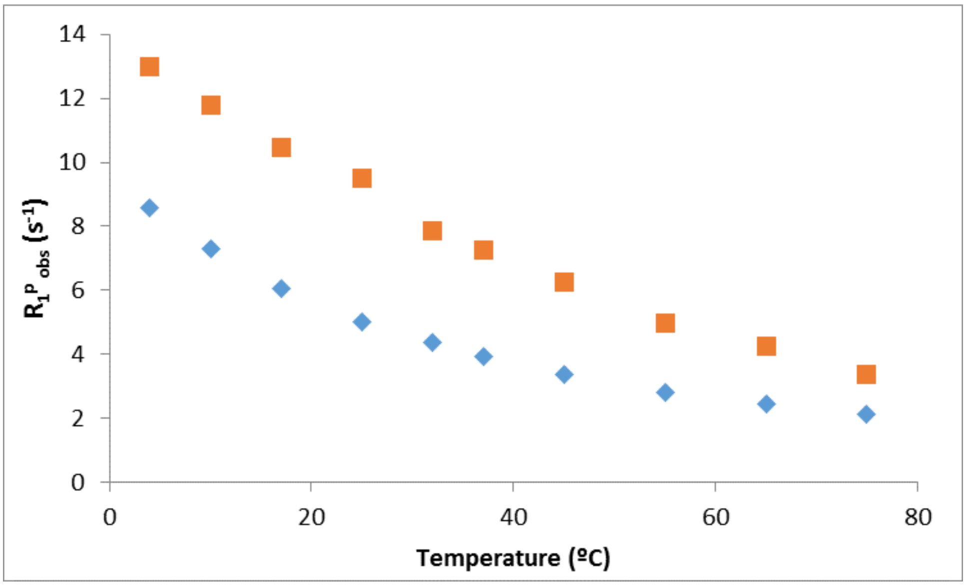

Figure SI1. Temperature dependence of the water proton longitudinal relaxation rate for Gd$\mathbf{L_1}$ (20 MHz, 1.0 mM pH 7.0 (■)) and for Gd$\mathbf{L_2}$ (20 MHz, 1.13 mM, pH 7.1(♦))

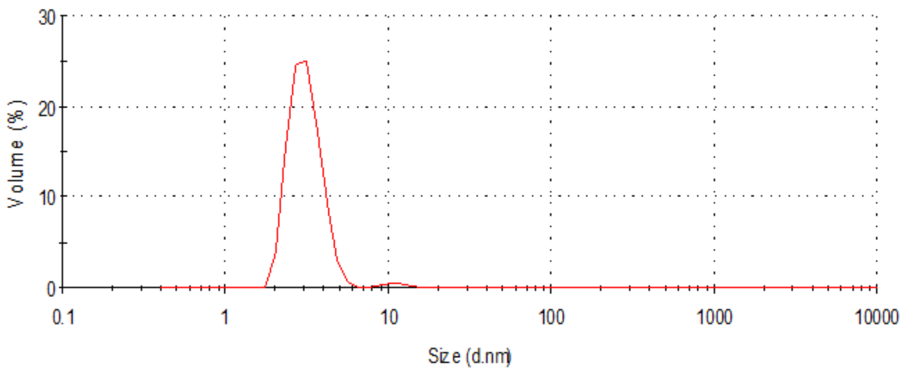

Figura SI2. Size distribution (%Volume) for Gd$\mathbf{L_2}$ (5.67 mM, pH 7.1, 25 ºC).

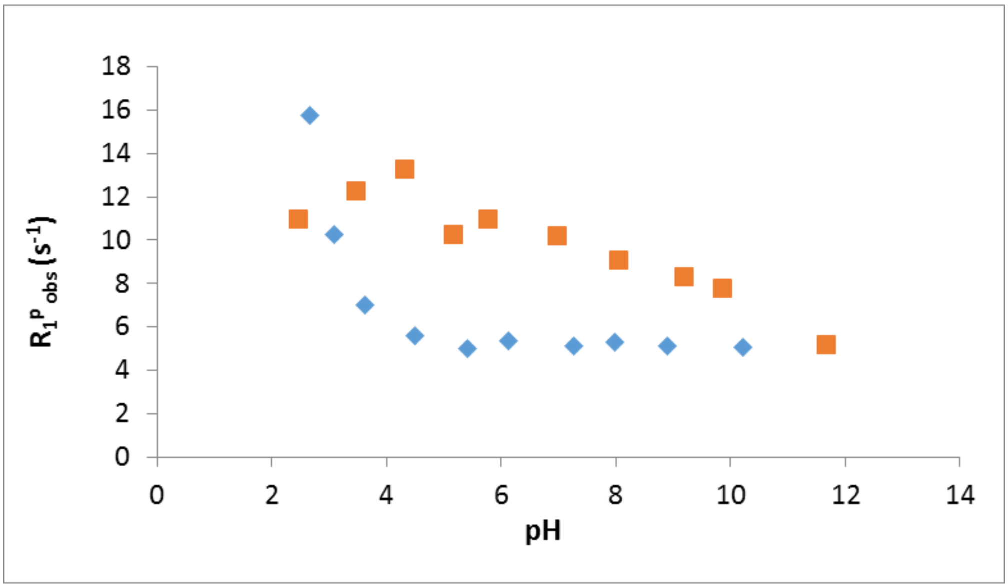

Figure SI3. pH dependence of the water proton longitudinal relaxation rate for Gd$\mathbf{L_1}$ (20 MHz, 1.0 mM, 25 ºC (■)) and for Gd$\mathbf{L_2}$ (20 MHz, 1.13 mM, 25 ºC (♦)).

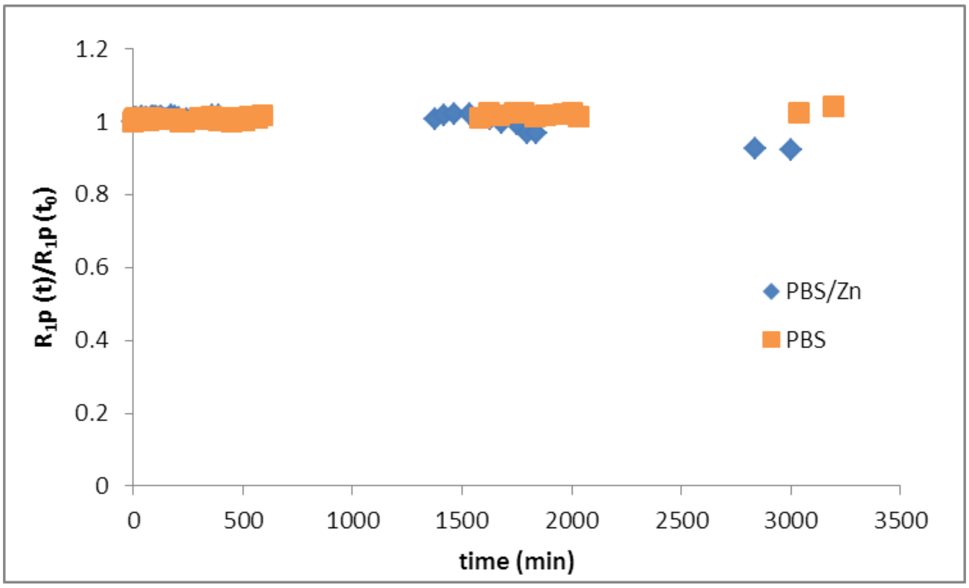

Figure SI4. Time evolution of the relative water proton relaxation rate *R1p*(t)/*R1p*(0) (20 MHz, 37 ºC) for a solution of Gd$\mathbf{L_2}$ (1.13 mM in PBS 2.5 mM, pH 7.1) (♦) and following addition of $ZnCl_2$ 0.75 mM (■).

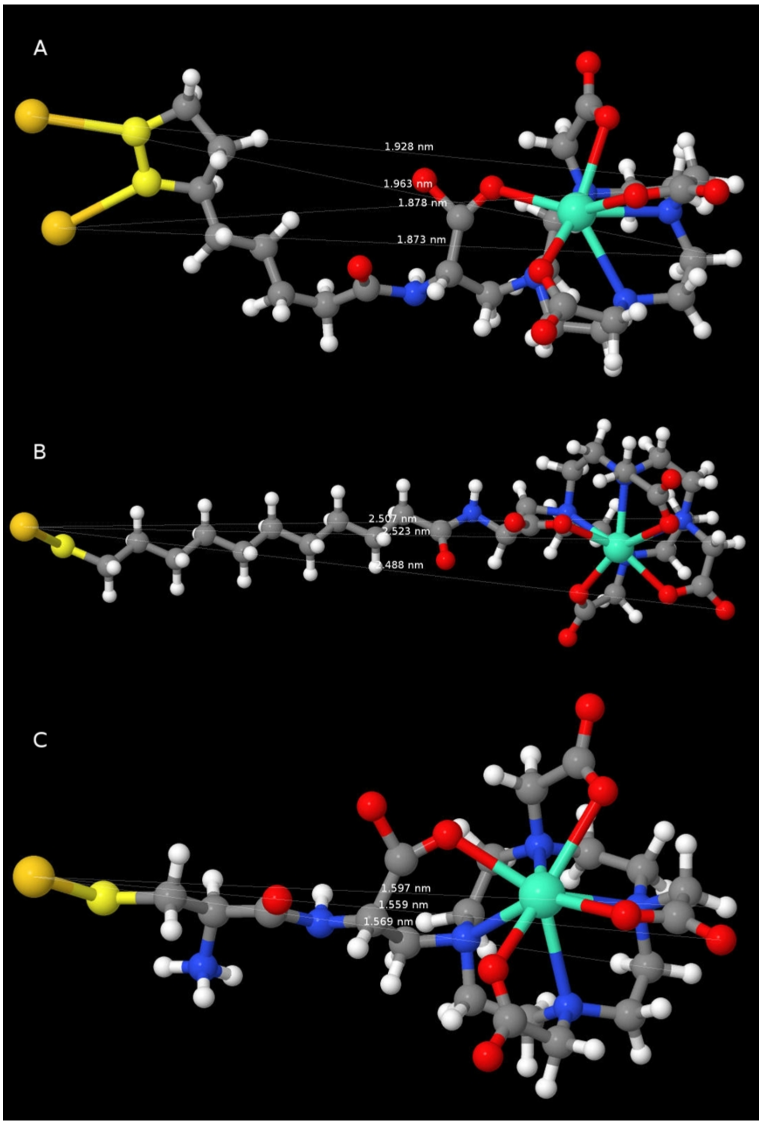

Figure SI5. Typical chelate length estimates from several Au…O and Au…H top-bottom distances measured over the optimized conformations of (A) Gd**L**$_1$, (B) Gd**L**$_2$ and (C) Gd**L**$_3$ obtained from PM6 semi-empirical calculations. Structures visualized with Jmol code [4].

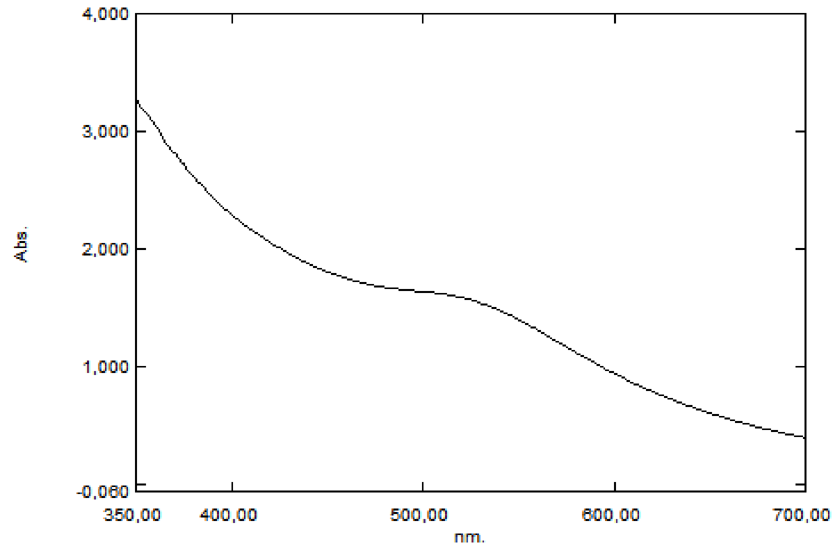

Figure SI6. UV-Vis spectrum of Gd$\mathbf{L_1}$@AuNPs.

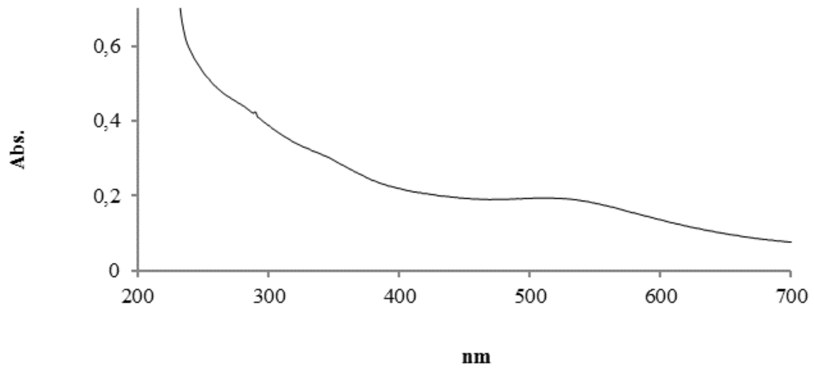

Figure SI7. UV-Vis spectrum of Gd$\mathbf{L_2}$@NPs.

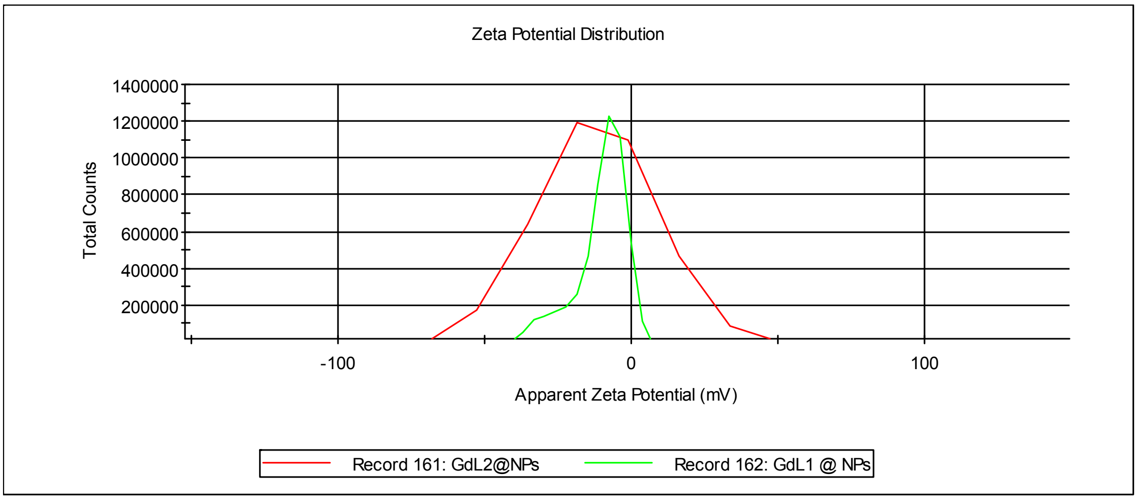

Figure SI8. Zeta potential distribution, expressed as total counts, for Gd$\mathbf{L_1}$@AuNPs (green line) and Gd$\mathbf{L_2}$@AuNPs (red line).

Table SI1. Zeta potencial for the Gd**L1**@AuNPs and Gd**L2**@AuNPs.

AuNPs	Zeta potential (mV)
Gd$\mathbf{L_1}$@AuNPs	-6.3
Gd$\mathbf{L_2}$@AuNPs	-13.7

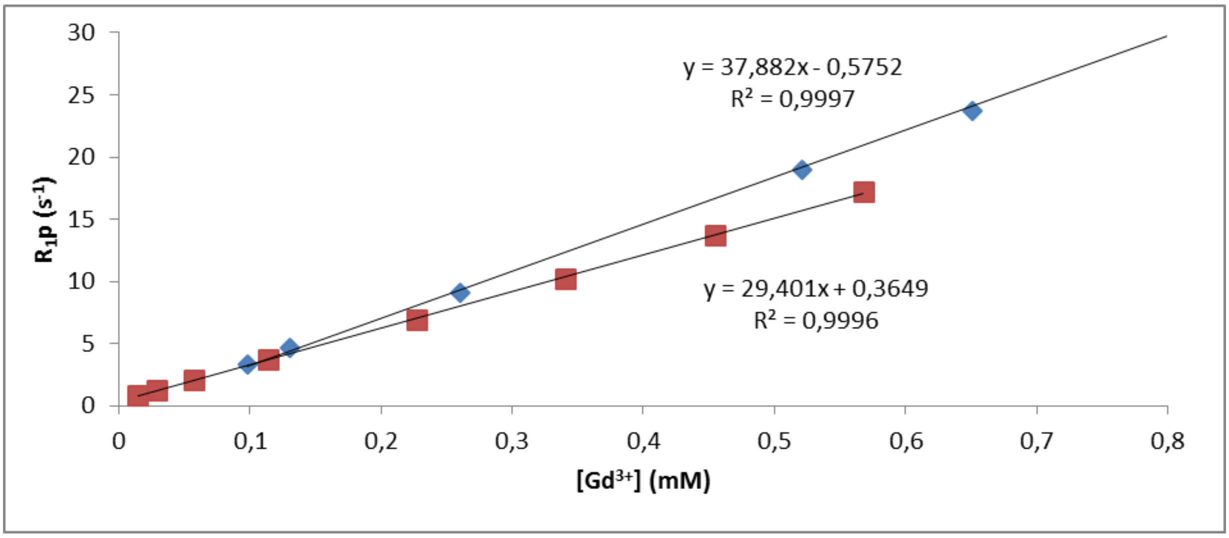

Figure SI9. Concentration dependence of the paramagnetic water proton relaxation rate R_{1p} ($R_{1p} = R_{1obs}$-R_{1d}) for Gd$\mathbf{L_1}$@NPs (■) and Gd$\mathbf{L_2}$ @NPs (♦) (20 MHz, 25 ºC, pH 7.1).

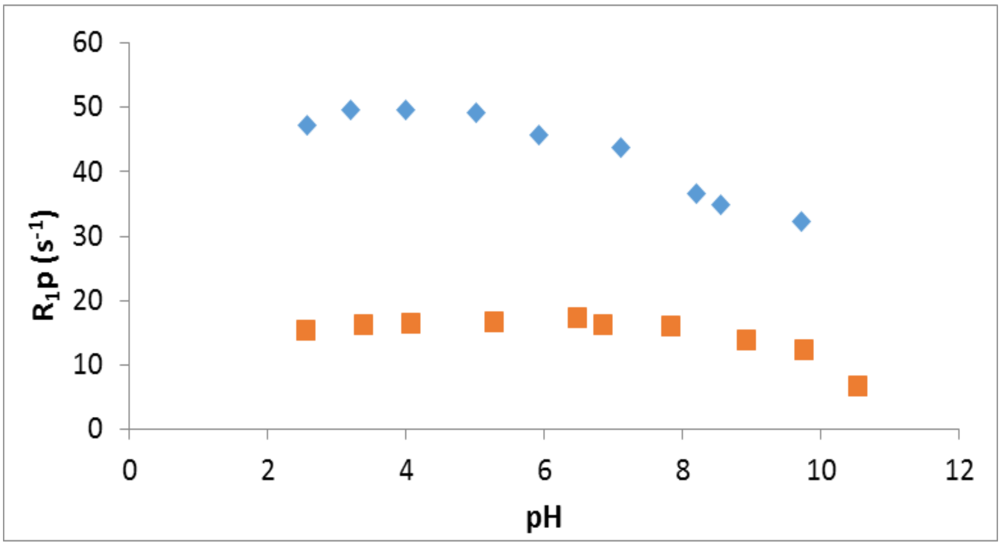

Figure SI10. pH dependence of the paramagnetic water proton relaxation rate for Gd$\mathbf{L_1}$@AuNPs (20 MHz, 25 ºC, 0.53 mM, (■)) and for Gd$\mathbf{L_2}$@AuNPs (20 MHz, 25 ºC, 1.30 mM (♦)).

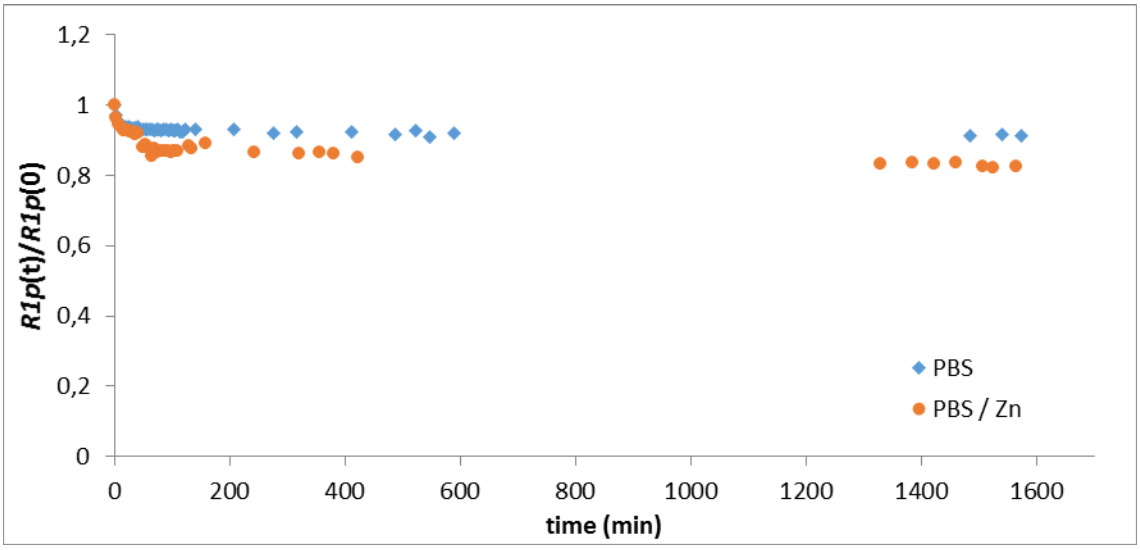

Figure SI11. Time evolution of the relative water proton paramagnetic relaxation rate *R1p*(t)/*R1p*(0) (20 MHz, 25 ºC) for a solution of Gd$\mathbf{L_1}$@NPs (0.53 mM in PBS 2.5 mM, pH 7.1) (♦) and following addition of 0.75 mM $ZnCl_2$ (●).

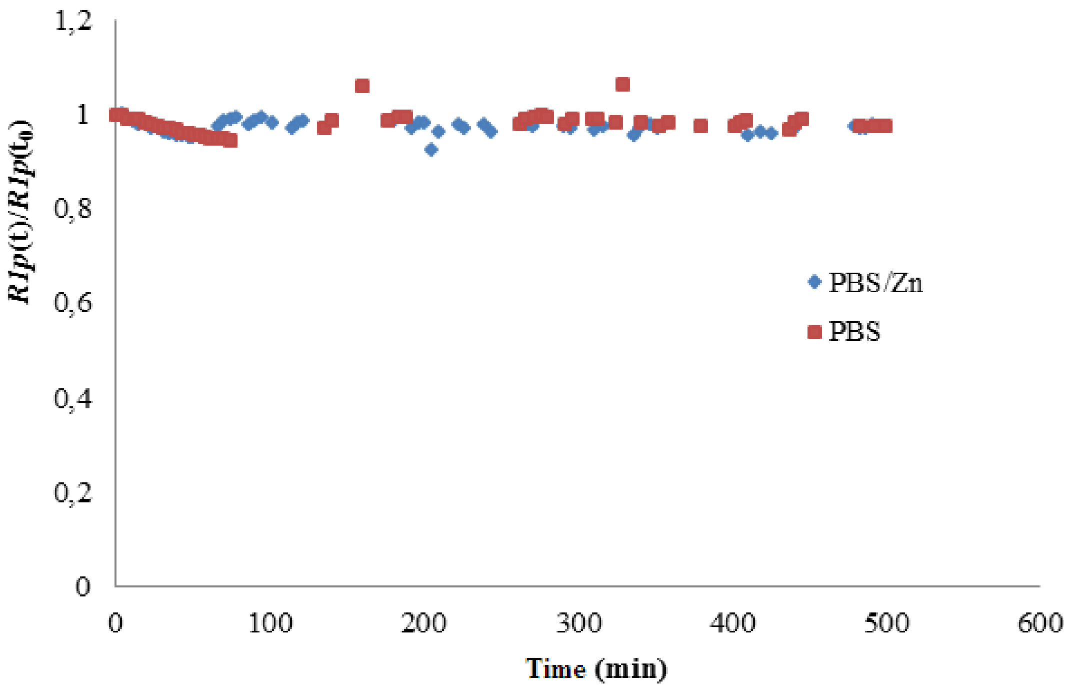

Figure SI12. Time evolution of the relative water proton paramagnetic relaxation rate *R1p*(t)/*R1p*(0) (20 MHz, 25 ºC) for a solution of Gd$\mathbf{L_2}$@AuNPs (1.30 mM in PBS 10 mM, pH 7.1) (■) and following addition of 0.75 mM $ZnCl_2$ (♦).

Table SI2. Characterization of Gd$\mathbf{L_1}$@AuNPs and Gd$\mathbf{L_2}$@AuNPs

	Gd$\mathbf{L_1}$@AuNPs^a	Gd$\mathbf{L_2}$@AuPs^a	Gd$\mathbf{L_3}$@AuNPs^b
[Gd] (mM) ([Au]/[Gd])^c	0.57 (1.4)	1.30 (0.87)	1.24 (3.0)
HD (nm)^d	4.8	5.9	3.9
Chelate length (nm)^e	1.9	2.5	1.6^f
Au core diam (nm)^g	1.0	0.9	0.7^f
Zeta potential (mV)	-6.3	-13.7	-12.3
N_{Au} core^h	31	23	11^f
N_{Chel}/NP^i	22^j	26^j	4^f
r_1 (mM^{-1} s^{-1}; 20 MHz, 25 ºC)	27	38	28
r_{1vol} (mM^{-1} s^{-1} nm^{-3}; 20 MHz, 25 ºC)^k	-	-	13

^{a}The synthesis and characterization of $\mathbf{L_1}$, $\mathbf{L_2}$, Gd$\mathbf{L_1}$, Gd$\mathbf{L_2}$ and Gd$\mathbf{L_1}$@AuNPs and Gd$\mathbf{L_2}$@AuNPs is described in this work.

^{b}The synthesis and characterization of $\mathbf{L_3}$ and Gd$\mathbf{L_3}$@AuNPs was described before [1].

^{c}The concentration of Gd and Au on the NPs solutions was determined by ICP-OES following digestion of the NPs with *aqua regia*.

^{d}The hydrodynamic diameter (HD, nm) of the NPs was measured by DLS.

^{e}The length of Gd$\mathbf{L_1}$ and Gd$\mathbf{L_2}$ was estimated by PM6 semi-empirical calculations for the most provable distended conformations (Figure SI5).

^{f}The length of Gd$\mathbf{L_3}$ was estimated by PM6 semi-empirical calculations for the most provable distended conformation, affording a revised value of 1.6 nm comparing to previous estimates of 1 nm [1].

^{g}The diameter of the gold core was estimated by taking into account the hydrodynamic diameter of the NPs measured by DLS, and the thickness of the chelate monolayer: $Au_{core} = HD\text{-}2\text{x}\mathrm{Chel}_{lenght}$

^{h}The number of Au atoms in the NPs core (N_{Au}= 30.9D^3) was calculated from the diameter of the metal core (D, nm) [2].

^{i} The number of immobilized complexes was calculated from the number of Au atoms in the core and the ratio Au/Gd obtained by ICP-OES.

^{j}A low ratio Au/Gd has obtained by ICP-OES for GdL_1@AuNPs (1.40) and especially for GdL_2@AuNPs (0.87) comparing to GdL_3@AuNPs (3.0) [1]. The number of immobilized chelates (22 and 26 chelates for GdL_1@AuNPs and GdL_2@AuNPs, respectively), calculated from the number of Au atoms in the metal core and the ratio Au/Gd), suggests the formation of a loosely bound second chelate layer around the NPs. This possibility deserves future investigation.

[k]The volumetric density of relaxivity was calculated using the relaxivity per NP and the HD diameter of the naoparticles: $r_{1\text{vol}}= (N_{chel} \text{ x } r_1)/4/3\pi(HD/2)^3$ [3]

References:

1. Ferreira, M. F.; Mousavi, B.; Ferreira, P. M.; Martins, C. I. O.; Helm, L.; Martins, J. A.; Geraldes, C. F. G. C., Gold nanoparticles functionalised with stable, fast water exchanging Gd3+ chelates as high relaxivity contrast agents for MRI. *Dalton Trans.* **2012,** *41* (18), 5472-5475.
2. Liu, X.; Atwater, M.; Wang, J.; Huo, Q., Extinction coefficient of gold nanoparticles with different sizes and different capping ligands. *Colloids Surf. B* **2007,** *58* (1), 3-7.
3. Bruckman, M. A.; Yu, X.; Steinmetz, N. F., Engineering Gd-loaded nanoparticles to enhance MRI sensitivity via T(1) shortening. *Nanotechnology* **2013,** *24* (46), 462001.